AN INVESTIGATION OF THE ANOMALOUS ATTITUDE MOTION OF THE ISEE-B SPACECRAFT

Richard W. Longman
Columbia University
New York, N.Y. U.S.A.

J. Andre Massart
European Space Operations Centre
Darmstadt, W. Germany

ABSTRACT

The ISEE-B spacecraft is a spin stablized satellite (19.8 rpm) with two radial 14.5 meter tape or ribbon booms having small tip masses. The limited sensor data concerning satellites attitude motion exhibits an unexpected persistent fluctuation of the spin rate with a 13.2 sec period (nearly 4.37 spin periods). Attempts were made to eliminate this spin ripple using a sequence of attitude manoeuvres designed for this purpose, and the ripple amplitude decreased to one third, only to return to its original value within roughly 10 days. The available data as well as the parameters of the spacecraft are given. Spin rate data for the spacecraft although somewhat inconclusive does not appear to have a persistent decay, so that one is led to seek an external source of energy to drive the ripple oscillations. The environmental forces affecting the satellite are reviewed, and solar radiation pressure identified as the most likely cause. The equations of motion for the ISEE-B satellite, subject to this pressure, are derived. Due to the very small amount of damping in the system and the nonlinear nature of the excitation, difficulties are encountered is isolating any steady oscillations or limit cycles, either analytically or numerically, in order to predict the spin ripple. Although the numerical results are not conclusive they suggest that solar radiation pressure alone is not sufficient to explain the spin ripple phenomenon.

Keywords: Attitude Dynamics, Solar Radiation Pressure, Flexible Spacecraft, Spin Stabilization.

1. INTRODUCTION

One of the most fascinating aspects of the history of man-made satellites is the history of unexpected or anomalous attitude behaviour. The first such satellite was also the first U.S. satellite Explorer I, which was thought to be spin stabilized about the axis of least moment of inertia, and yet its coning angle grew to 60° within a few hours of launch. Other spin stabilized satellites have unexpectedly spun up or despun (for example, Explorer XII and XX, Alouette I, Timation, ISIS I, etc., see Refs. 1 - 4). Spin rate fluctuations are also observed that are due to spacecraft temperature changes and associated thermal expansion resulting from earth reflected sunlight (Ref. 5). Gravity gradient satellites employing STEM booms have unexpectedly tumbled after coming out of the earth's shadow (Ref. 6), and certain dual spin satellites have exhibited a host of unexpected phenomena such as limit cycles, trap states, and phase locks (Ref. 7). Satellites with active attitude control systems have used all their attitude control fuel within a short period due to failure to model spacecraft flexibility. Reference 8 presents a nice history of some of these phenomena.

The subject of the present paper is the anomalous spin behaviour of the ISEE-B spacecraft, a nearly symmetric satellite with two radial 14.5m tape booms Rather than showing a secular spin up or down as in some of the above satellites, this spacecraft exhibits a persistent small oscillation of the spin rate. When an attitude manoeuvre was devised and used to decrease this spin ripple, it unexpectedly returned to its original amplitude within a matter of days. Luckily the amplitude is sufficiently small that the spin ripple does not interfere with the mission objectives, although it does adversely affect the attitude reconstruction.

2. THE ISEE-B SPACECRAFT

The ISEE-B spacecraft is part of an international program between NASA and ESA using three spacecraft, a mother/daughter pair (ISEE-A/ISEE-B) launched by the same rocket on 22 October 1977 into nearly identical highly eccentric earth obits, and an interplanetary spacecraft (ISEE-C) launched a few months later into an orbit about the unstable sun/earth-moon libration point between the sun and the earth. The separation between the ISEE-A and ISEE-B satellites is controlled by orbital manoeuvres of the lighter ISEE-B. Mission attitude requirements dictate that the ISEE-B spin axis be kept perpendicular to the ecliptic plane and that the spin rate be controlled to within narrow limits. Table 1 lists the nominal orbit and attitude parameters.

The geometrical structure of the spacecraft is illustrated in Figure 1. The central hub is a cylinder with solar cells mounted on the circumference except for a skirt at the bottom where scientific instruments are placed and three hard booms containing scientific equipment are hinged. Symmetrically connected to the spacecraft are two 14.5 m long tapes serving as an experiment RF antenna. Table 2 lists the basic data related to the geometrical, thermal, and mass properties of the satellite.

Proc. Int. Symp. Spacecraft Flight Dynamics, Darmstadt, FRG, 18-22 May 1981 (ESA SP-160, Aug. 1981)

With this configuration it is clear that the in-orbit manoeuvres induce oscillations of the wires in the centrifugal force field. All information on attitude motion and wire oscillation must be deduced from the data of a combined sun-earth albedo sensor. This sensor consists of two slits with $120^{\circ} \times 1^{\circ}$ fields of view. One of the slits is mounted in a satellite meridian plane. The other, inclined at an angle of 30° intersects the meridian slit at the satellite equator. During each spin revolution both slits detect the sun, and the associated transit times, obtained from a 4096Hz clock, are loaded into a 16 bit register. The clock recycles every 65536 counts (16 sec). When the telemetry down link is operating in the highest bit rate (8192 bps), successive transit times of the sun in both the meridian and oblique slits are available. The difference between successive sun crossings in one of the slits can be used as the spin period, and the solar elevation with respect to the spacecraft equator can be derived from the difference in transit times in the meridian and inclined slits.

3. THE SPIN RIPPLE PHENOMENON

Table 3 gives typical raw sensor data from which the attitude behaviour is deduced. The data show that the sun elevation stays constant at -53 counts (2.7° below the equator) with an isolated count of -52. This constant elevation excludes the possibility of any nutation of the spin axis greater than 0.05°, which is indicative of the presence on board of a well tuned nutation damper The data also show that the spin period varies between 12414 counts (3.031 sec) and 12434 counts (3.036 sec), and this is the spin ripple.

Studying more closely the spin period data reveals that they can be fitted well by a sine wave having a period of about 4.37 times the average spin period. For a nominal spin period of 3.03 sec, the spin ripple period is estimated to be 13.24 sec (Ref 10,11).

This oscillation in the spin of the hub must be accompanied by oscillation of the flexible tapes. If the flexibility is modelled by assuming the tapes to be rigid but hinged at the base, then there are five spacecraft vibration modes as shown in Figure 2 (Ref.12). The equatorial anti-symmetric mode involves rotation of each tape in the same direction, and a corresponding rotation of the hub in the opposite direction (indicated by the bold arrow). It is this mode which is excited during spin ripple. The equatorial symmetric mode involves only translational motion of the hub and hence cannot be observed from the on board sensors. Similarly, the meridian symmetric mode involves hub translation along the spin axis without rotation of the hub and hence it too is unobservable. Both the meridian anti-symmetric mode and the nutation mode involve coning motion of the hub, the former is of higher frequency and in the latter the tapes remain approximately perpendicular to the coning axis. The constant elevation angle observed in the data indicates that the amplitudes of these two modes is negligible.

Reference 13 describes the strategy followed by ESOC to reduce the amplitude of the spin ripple, taking into account the numerous practical constraints imposed by the on board control system as well as the ground operations. The main constraints are :

i) The on board system quantizes the start/stop times of a spin rate change torque to 0.5 sec corresponding to a spin ripple phase shift of 13-14 deg.

ii) Consecutive spin up/spin down torque pulses must be separated by at least 20-30 sec (about two spin ripple periods).

iii) The spin period must be kept within tight limits (3.03 ± 0.015 sec).

The main features of the procedure applied for each spin ripple damping exercise are as follows:

i) The telemetry down link is switched to the high bit rate and attitude data are collected.

ii) the spin ripple amplitude, phase and frequency are estimated by a least squares fit of the sun transit times in the meridian slit.

iii) A dynamic simulation predicts the spin ripple for a sufficient number of cycles into the future to generate a sequence of spin up/spin down control torques optimized to fit the pulses near the extreme value of the spin ripple oscillation.

iv) The telecommands are generated and uplinked to the satellite.

Figure 3 illustrates the outcome for the first spin ripple damping manoeuvre which reduced the spin ripple amplitude to approximately one third its original value. Two such manoeuvres were performed in October 1979 and April 1980. On both occasions it was observed that within a week to 10 days the spin ripple amplitude returned to its original value, as is illustrated in Figure 4. In normal operation, the attitude data obtained is insufficient to study the spin ripple phenomenon. During two additional periods, October 1979 and February 1981, the telemetry down link was switched to the high bit rate for various periods, and the results are shown in Figure 5. In the top part of the figure the high bit rate was used for five minutes every four hours during one orbit, and in the lower part of the figure the data were taken for five minute intervals at a sequence of times clustered at the beginning and ending roughly once every orbit.

It is clear from the data that the spin rate oscillation of $\pm$ 10 clock units (1 clock unit = 0.24 msec.) amplitude remained essentially constant over the period of the test and was nearly equal to the value obtained some 10 days after the end of the spin ripple damping manoeuvres, in spite of the satellite manoeuvre occuring in between, orbital evolution, variation in instantaneous distance from the earth, etc. It is the aim of this paper to investigate the cause of the spin ripple, and the reason for its persistent return to its steady state value after the damping manoeuvre.

4. APPROACH TO THE PROBLEM

In order to try to isolate the cause of the spin ripple the following chain of heuristic reasoning was employed.

1) The amplitude of the oscillation of the tape booms associated with the ripple is about 3.0°, and the amplitude of the oscillation in the hub spin angle itself is about 0.31° ($\pm$ 10 clock units adjusted for the inherent averaging over a spin period of the sun transit information). These numbers are sufficiently small that a linear model of the spacecraft dynamics would be well justified.

2) The system contains damping as a result of flexing (bending and longitudinal stretching due to variations of centrifugal force during oscillations, Ref. 12), and this damping is continually acting during spin ripple oscillations.

The energy needed to maintain the oscillations must come from somewhere. If it is within the system, energy would continually be transferred from spin into spin ripple. The data are somewhat inconclusive, but do not appear to exhibit the long term despin trend needed for this. Hence, one is led to postulate an external source for this energy. The external source might be a nonlinear function of the variables of the system, making the differential equations nonlinear.

3) Consider for the moment an equation of the form

$$\ddot{\alpha} + 2c\dot{\alpha} + \omega_{\alpha}^{2}\alpha = f(t)$$

which can represent any of the modes of the dynamic model. The f(t) is used to represent the inputs to the mode coming from the energy source of interest. Of course, these inputs will probably be a function of the state of the system, and perhaps a nonlinear one, but if we know the actual periodic ripple motion, it could be substituted into the approximate expression to obtain f(t), and then the solution for α of the above differential equation would have to be the appropriate modal component of the ripple motion.

4) Let the above equation be written in operator form $L(\alpha) = f(t)$. The solution is a sum of a particular solution α_p and the solution to the homogeneous equation α_H. If $\alpha^{(1)}$ and $\alpha^{(2)}$ are any two solutions corresponding to two different initial conditions, then $L(\alpha^{(1)}) = f$, $L(\alpha^{(2)}) = f$ and therefore $L(\alpha^{(1)} - \alpha^{(2)}) = 0$. Thus the difference between any two solutions satisfies the homogeneous equation. Since the differential equation is stable, this α_H approaches zero with increasing time so that all solutions converge to one particular solution (in this case a periodic particular solution), and α_H which contains the natural frequency of the system disappears from the solutions. The spin ripple frequency appears to be at or near one of the mode frequencies of the system, and hence this frequency must somehow be contained in the particular solution

5) The f(t) obtained as a linear or nonlinear function of the state and time for this oscillatory ripple motion, can be written as the sum of sinusoids with a fundamental frequency and in the case of a nonlinearity, sums and differences of the frequencies in the system (e.g. the product of two sinusoids is the sum of sinusoids with frequencies that are the sum and difference of the original frequencies). For any (completely) damped linear system $L(\alpha) = f(t)$ if f(t) is $\sin\omega t$ (or a sum of sinusoid), then the α_p solution is of the form $M\sin(\omega t + \phi)$ (or a sum of such terms), where M and ϕ depend on ω. Therefore, if the long term solution (after the transients α_H have died away) contains the natural frequency of the system, this frequency must be present in the driving function f(t), and the excitation force on the spacecraft must generate this frequency in f(t).

6) From the rise time after the spin ripple manoeuvre (Figure 4), as well as Ref. 12, it appears that the time constant (i.e. $1/c$) of the system is somewhere in the neighbourhood of six days. If the input f(t) is an oscillation at the resonant frequency, $F\cos\omega_{\alpha}t$ with amplitude F, then the solution to the equation is an oscillation at the same frequency with amplitude $(1/c)F$. Converting to consistent units shows that the gain factor $1/c$ between input and output amplitudes is on the order of 518,400. Hence, the external force that produces f(t) with some component at frequency ω_{α} can be very small indeed and still produce an oscillation of the observed 3.0° amplitude. If the ripple frequency is not at or very close to a resonant frequency, the gain would be much lower.

7) The external forces or sources of energy for an orbiting satellite include :

Solar radiation pressure
Radiative heating
Gravity gradient torques
Atmospheric drag
Magnetic field interactions

Any one of these acting alone can significantly influence the attitude dynamics of a satellite. For example, the magnetic field interactions include torques resulting from induced eddy currents, V x B induced current, and magnetic hysteresis effects (Ref. 3); radiative heating can produce thermal expansions that generate nutation (Ref. 14), or change the spin rate (Ref. 5); and structural energy dissipation due to gravity gradient induced deformations can despin a spacecraft (Ref. 15). Often the anomalous behaviour of a satellite is due to a coupling between two or more of these inputs. The solar motoring that caused spin up or spin decay of many satellites is associated with distortion due to solar radiative heating (with a phase lag) and solar radiation pressure (Ref. 2). Such distortions can also interact with atmospheric drag in essentially the same manner (Ref. 16). Obviously, there is a great wealth of possible combinations, and there is always room for more interaction effects.

Consider how these forces relate to the ISEE-B spacecraft. Its orbit shown in Table 1 includes a perigee altitude of 1900 km, an apogee altitude of 137,000 km, and an orbital period of 2.4 days. For such an orbit atmospheric drag can be eliminated from the list of possible causes. Due to the high orbital eccentricity, gravity gradient torque and magnetic field interactions will have a relatively strong effect only over a short time in each orbit. With a time constant of about 6 days a periodic increase in the ripple at each perigee followed by decay should be observed in the data if either of these forces were the culprit. Examining Figures 4 and 5 shows no such behaviour.*

This leaves only the two sun related inputs. Nominally, the spin axis is maintained perpendicular to the ecliptic plane so that the tape booms are completely shadowed for some period of each revolution. It is unfortunatethat no spin ripple data is available for the few periods for which the sun angle was such that only partial shadowing occurred. This could have firmly established the correlation with solar inputs.

Let us consider whether thermal distortions alone could produce the ripple. Thermal inputs from earth reflected energy imply a perigee dependence in the data* which is not observed so that only solar radiative heating need be considered. Thermal effects alone were responsible for the tumbling of certain gravity gradient satellites. The mechanism required differential heating of the unzippered STEM booms whose complex geometry allows a component of bending, due to thermal expansion, perpendicular to the direction of the incident sunlight, and this couples with boom structural dynamics to produce a coning motion after sudden input of heat energy. The very simple geometry of the berylium-copper tapes with a thickness of only 0.0004 m, illuminated in the plane of rotation seems to preclude any important thermal bending effects. This leaves only thermal expansion. Periodic thermal expansion of the spacecraft can produce some fluctuations of the spin rate due to change in inertia.*

The above considerations leave only solar radiation pressure as the cause of the spin ripple. The fact that the radiation pressure impinges at a 90° angle of incidence onto the full surface of each light tape twice during each spacecraft rotation makes this a likely source of the needed energy to drive the spin oscillations.

8) The observed data, for example in Figure 3, forms a rather clean sine wave, but the actual tape boom motion could be quite complex. The spin rate information is obtained by taking the difference in sun transit time as a period of rotation that applies to the midpoint of the time interval, then the amplitude, phase and frequency of a sine wave are adjusted to achieve a fit. Finally, the amplitude is adjusted for the averaging inherent in the period information.

The amplitude of the spin ripple is $\pm$ 10 clock units, so that other frequencies beside the fundamental one can be present in the dynamics if their effect on the period is less than a clock unit. Also, the sampled nature of the data implies that oscillations at the spin frequency or its multiples can never be observed, although by studying the nature of the solar radiation pressure it is clear that such oscillations must exist. Furthermore, the tape oscillations associated with all unobservable modes will not appear in the data.

Let us consider what modes could be present in the spin ripple dynamics. Since there is no nutation, neither the meridian anti-symmetric nor the nutation mode can be present. The meridian symmetric mode could be present since it is unobservable. This motion would necessitate twisting of the tapes near the base, and the solar radiation pressure impinging on a twisted tape would have a force component inthe meridian plane which could feed these oscillations, and the equatorial force components would feed one or both equatorial modes. One can imagine some type of coning motion of boom developing as a result of twisting, induced by initial condition excitation of the meridian symmetric mode, and radiation pressure coupling. Such a mechanism is reminiscent of the solar thermal excitation of the STEM booms that tumbled gravity gradient satellite (Refs. 6, 17). The small width of the tape (0.005 m) makes this mechanism seem unlikely. Also, the meridian symmetric mode has never been excited by any thrust manoeuvre (although precession manoeuvres have been performed which would excite the meridian anti-symmetric mode that also involves tape twisting), and it is not clear how the coupling with the equatorial symmetric mode could get a driving term of the 13.2 sec ripple frequency. To model the dynamics of this mechanism, and then determine whether it can predict the observed data is a formidable undertaking and will not be considered here.

The calculated period of the equatorial anti-symmetric mode is 12.76 sec, while that of the equatorial symmetric mode is 13.47 sec. The observed spin ripple frequency is 13.2 sec. If the spin ripple is occuring at one of the modal frequencies, presumably it would be the equatorial anti-symmetric mode which must be excited in the ripple. Nevertheless, the observed frequency is closer to that of the equatorial symmetric mode. The only way that the ripple could correspond to this mode is if the mode were for some reason observable, for example, if there was a significant centre of mass imbalance (there are in fact unequal tip masses). An imbalance would also couple the two equatorial modes making the oscillations more observable from the sensors. The equatorial symmetric mode is excited every revolution by the solar radiation pressure, whereas the equatorial anti-symmetric has no direct forcing term. On the other hand, if the ripple is a limited cycle it need not be at either modal frequency, but due to the very

*Although there is no clear evidence of spin ripple dependence on perigee, after the study reported here was completed, some spin rate data were found that correlated with perigee crossings. As a result thermal expansion as well as other perigee-related effects will now be investigated.

small damping, and the small excitation available from solar radiation it should still be quite close to a resonant frequency in order to obtain the amplitudes observed. A limit cycle requires a nonlinear differential equation , and the solar radiation pressure involves an absolute value which is nonlinear and couples the two equatorial modes.

5. EQUATIONS OF MOTION FOR RADIATION PRESSURE EXCITATION

Based on the reasoning of the previous section, the equations of motion for the ISEE-B spacecraft were developed considering solar radiation pressure forces only, assuming specular reflection from the tapes, and modelling the tapes are rigid physical pendula hinged at their base. This latter assumption models the lowest frequency vibration mode of the tapes with reasonable accuracy. Only equatorial planar motions are considered.

5.1 Notation

With reference to Figure 6, define an inertial coordinate system centered at O with axes $\hat{I}_1, \hat{I}_2$ with $\hat{I}_2$ being parallel to the incident sunlight (assumed inertially fixed in direction). Define axes $\hat{h}_1, \hat{h}_2$ fixed in the hub and centered at its geometric centre, H, assumed also to be its centre of mass. The generalised coordinates used, $q_1, q_2, q_3 \cdots q_5$ are X_1, X_2 specifying the inertial position of the hub centre $\underline{R}_{OH} = X_1\hat{I}_1 + X_2\hat{I}_2$ Θ specifying the angular orientiation of the hub, and angles α_1 and α_2 for deflection of the tapes. In terms of these variables, α_1 and α_2 where

$$\alpha_1 = \alpha_1 + \alpha_2 \quad ; \quad \alpha_2 = \alpha_1 - \alpha_2$$

represent modal variables for the equatorial anti-symmetric and equatorial symmetric modes respectively.

Introduce the following nomenclature and constants.

Mass related parameters:

- m_h = mass of hub including hinge booms
- m_t = mass of tip mass (both assumed to be of equal mass)
- ρ = mass per unit length of tape booms
- ℓ = length of tape booms
- m = $\rho\ell$, mass of tape boom
- M = $m_h + 2m + 2m_t$, total spacecraft mass

Inertia related parameters:

- I_h = hub and hinge boom moment of inertia about spin axis (tape boom mass removed)
- r = $|\underline{R}_{HB}|$ radius from spin axis to base of tape booms
- $M_3 = (m_t + 1/3\, m)\ell^2$
- $M_2 = (m_t + 1/2\, m)\ell$
- $M_1 = M_3 + rM_2$
- $I = I_h + [2M_3 + 4rM_2 + 2(m_t + m)r^2]$ = inertia of total satellite about spin axis if satellite were rigid

Radiation pressure related parameters:

- P = solar pressure constant
- β = reflectivity of berylium-copper tape booms
- w = width of tape booms
- $\mathcal{P} = w(1+\beta)P$, maximum force per unit length on tape
- P_H = total force due to radiation pressure on hub (includes averaged force on hing booms)
- ℓ_i^* = length of shadow on boom i

Time variables:

- t = true time
- ω = nominal spin angular velocity
- $\tau = \omega t$,scaled time

Frequency parameters:

- $\omega_{\alpha_1} = \omega_1 \omega$ angular frequency of equatorial anti-symmetric mode
- $\omega_{\alpha_2} = \omega_2 \omega$ angular frequency of equatorial symmetric mode
- $\omega_1 = \left[rM_2/(M_3 - 2M_1/I)\right]^{1/2}$
- $\omega_2 = \left[(rM_2 + 2M_2^2/M)/(M_3 - 2M_2^2/M)\right]^{1/2}$

5.2 Basic Formulation

Newtons law for a differential mass element dm located relative to an inertially fixed point by vector $\underline{R}ov$ is

$$d\underline{F} = \ddot{\underline{R}}_{ov}\, dm$$

where the time derivative is taken relative to inertial coordinates, and $d\underline{F}$ is the differential force applied to dm. Vector $\underline{R}ov$ is a function of the five generalized coordinates $q_j : X_1, X_2, \Theta, \alpha_1, \alpha_2$. The directions $\partial\underline{R}_{ov}/\partial q_j$ are associated with directions of motion allowed by the constraints of the system. Taking the dot product of the above equation with these five directions and integrating over all mass in the system, $\mathcal{M}$, gives

$$\int_{\mathcal{M}} \frac{\partial \underline{R}_{ov}}{\partial q_j} \cdot d\underline{F} = \int_{\mathcal{M}} \frac{\partial \underline{R}_{ov}}{\partial q_j} \cdot \ddot{\underline{R}}_{ov}\, dm$$

$$= \int_{\mathcal{M}} \left[\frac{d}{dt}\frac{\partial}{\partial \dot{q}_j}\left(\tfrac{1}{2}\dot{\underline{R}}_{ov}\cdot\dot{\underline{R}}_{ov}\right) - \frac{\partial}{\partial q_j}\left(\tfrac{1}{2}\dot{\underline{R}}_{ov}\cdot\dot{\underline{R}}_{ov}\right)\right] dm$$

$$= \frac{d}{dt}\frac{\partial T}{\partial \dot{q}_j} - \frac{\partial T}{\partial q_j}$$

where $\partial\underline{R}_{ov}/\partial q_j = \partial\dot{\underline{R}}_{ov}/\partial\dot{q}_j$ has been used, and

$$T = \int_{\mathcal{M}} \tfrac{1}{2}\dot{\underline{R}}_{ov}\cdot\dot{\underline{R}}_{ov}\, dm$$

is the total kinetic energy of the system, and let

$$Q_j = \int_{\mathcal{M}} \frac{\partial \underline{R}_{ov}}{\partial q_j}\, d\underline{F}^e \qquad (1)$$

be the generalised force associated with variable q_j. Here superscript **e** has been introduced on $d\underline{F}^e$ to indicate that only external forces need be considered since internal forces will cancel due to Newton's third law. Each integral can be separated into five integrals, one each for the hub, for each tape boom, and for each tip mass.

Since there will be energy dissipation due to boom motion let the force associated with it be introduced using a Rayleigh dissipation function

$$\mathcal{J} = \tfrac{1}{2}c\dot{\alpha}_1^2 + \tfrac{1}{2}c\dot{\alpha}_2$$

with c being the appropriate damping constant. Then the equations of motion are

$$Q_j = \frac{d}{dt}\left(\frac{\partial T}{\partial \dot{q}_j}\right) - \frac{\partial T}{\partial q_j} + \frac{d\,\mathcal{F}}{d\dot{q}_j} \qquad (2)$$

The next sections evaluate the five integrals for T and for each Qj.

5.3 Kinetic Energy Calculation

The kinetic energy of the hub is the sum of the kinetic energy of translation of the centre of mass as if the hub were a point mass, and the kinetic energy of rotation about the centre of mass:

$$T_h = \tfrac{1}{2} m_h (\dot{X}_1^2 + \dot{X}_2^2) + \tfrac{1}{2} I_h \dot{\theta}^2$$

In order to obtain the kinetic energy of a tape, consider a differential element of length dq with mass $dm = \rho\, dq$ and located at distance $q = |\underline{R}_{BV}|$ along boom 1 (see Figure 6). The inertial position vector to this mass and its inertial derivative are

$$\underline{R}_{OV} = X_1 \hat{i}_1 + X_2 \hat{i}_2 + r\hat{h}_1 + q\hat{b}_1^1$$

$$\dot{\underline{R}}_{OV} = \dot{X}_1 \hat{i}_1 + \dot{X}_2 \hat{i}_2 + r\dot{\theta}\hat{h}_2 + q(\dot{\theta}+\dot{a}_1)\hat{b}_2^1$$

Then the kinetic energy of boom 1 is

$$T_{b_1} = \int_0^{\ell} \Big[\tfrac{1}{2}(\dot{X}_1^2+\dot{X}_2^2) + \tfrac{1}{2} r^2\dot{\theta}^2 + \tfrac{1}{2} q^2(\dot{\theta}+\dot{a}_1)^2 + r\dot{\theta}(-\dot{X}_1\sin\theta + \dot{X}_2\cos\theta) + rq\dot{\theta}(\dot{\theta}+\dot{a}_1)\cos a_1 + q(\dot{\theta}+\dot{a}_1)(-\dot{X}_1\sin(\theta+a_1) + \dot{X}_2\cos(\theta+a_1))\Big]\rho\, dq$$

which is easily integrated. The kinetic energy of tip mass 1 treated as a point mass is obtained by deleting the integral and replacing the ρ of the integrand m_t. Doing the same operations for boom 2 and adding the five kinetic energies gives the desired total kinetic energy:

$$\begin{aligned} T = {} & \tfrac{1}{2} M(\dot{X}_1^2+\dot{X}_2^2) + \tfrac{1}{2}(I_h + 2mr^2 + 2m_t r^2)\dot{\theta}^2 \\ & + \tfrac{1}{2}(m_t + \tfrac{1}{3}m)\ell^2\left[(\dot{\theta}+\dot{a}_1)^2 + (\dot{\theta}+\dot{a}_2)^2\right] \\ & + (m_t + \tfrac{1}{2}m) r\ell\,\dot{\theta}\left[(\dot{\theta}+\dot{a}_1)\cos a_1 + (\dot{\theta}+\dot{a}_2)\cos a_2\right] \\ & + (m_t + \tfrac{1}{2}m)\ell\Big\{(\dot{\theta}+\dot{a}_1)\left[-\dot{X}_1\sin(\theta+a_1) + \dot{X}_2\cos(\theta+a_1)\right] \\ & - (\dot{\theta}+\dot{a}_2)\left[-\dot{X}_1\sin(\theta+a_2) + \dot{X}_2\cos(\theta+a_2)\right]\Big\} \end{aligned} \qquad (3)$$

5.4 The Differential Force Due to Solar Pressure

Assuming specular reflection, the absorptivity is $1-\beta$ where β is the reflectivity. Let η be the angle between the perpendicular to the boom surface and the incident sunlight. The area of differential element dq of boom 1 projected onto a plane perpendicular to the incident light is $w\,dq\,|\cos\eta|$. Then the differential force on this element is given by

$$d\underline{F}^e = p(w\,dq|\cos\eta|)\Big\{(1-\beta)\sin\eta\,\hat{b}_1' + \left[(1-\beta)\cos\eta + 2\beta\cos\eta\right]\hat{b}_2'\Big\}$$

The component of radiation pressure along the tape (along $\hat{b}_1^1$) should have negligible influence on the dynamics and is dropped, so that the differential forces on boom 1 and boom 2 can be written as

$$\begin{aligned} \text{boom 1:}\quad & d\underline{F}^e = P|\cos(\theta+a_1)|\cos(\theta+a_1)\hat{b}_2'\,dq \\ \text{boom 2:}\quad & d\underline{F}^e = -P|\cos(\theta+a_2)|\cos(\theta+a_2)\hat{b}_2^2\,dq \end{aligned} \qquad (4)$$

These forces apply to each element dq that is not in the shadow of the spacecraft. In nominal satellite operation the sun direction is perpendicular to the spin axis and each boom becomes totally shadowed for part of each rotation and is partially shadowed for half of each rotation. When $\sin\theta \geq 0$ there is shadowing on boom 1 and the distance from the base of the shadow is ℓ_1^*. Boom 2 has shadow length ℓ_2^* and shadowing occurs when $\sin\theta < 0$. These lengths are given as

$$\ell_1^*(\theta,a_1) = \begin{cases} \min\left(\ell, \dfrac{r(1-|\cos\theta|)}{|\cos(\theta+a_1)|}\right) & \text{when } \sin(\theta) \geqslant 0 \\ 0 & \text{when } \sin\theta < 0 \end{cases}$$

$$\ell_2^*(\theta,a_2) = \begin{cases} 0 & \text{when } \sin\theta \geqslant 0 \\ \min\left(\ell, \dfrac{r(1-|\cos\theta|)}{|\cos(\theta+a_2)|}\right) & \text{when } \sin\theta < 0 \end{cases} \qquad (5)$$

The differential force due to radiation pressure on each boom applies from ℓ_i^* to ℓ.

5.5 The Generalized Force

Each generalized force Qj can be written as the sum of five integrals, one over each mass element of the system. The radiation pressure on the tip masses is negligible so that these two integrals can be set to zero. For the hub, $\partial\underline{R}_{OV}/\partial X_1 = \hat{i}_1$ and $\partial\underline{R}_{OV}/\partial X_2 = \hat{i}_2$ so that

$$\int_{hub} (\partial\underline{R}_{OV}/\partial X_1)\cdot d\underline{F}^e = \hat{i}_1 \cdot \int_{hub} d\underline{F}^e = 0$$

$$\int_{hub} (\partial\underline{R}_{OV}/\partial X_2)\cdot d\underline{F}^e = \hat{i}_2 \cdot \int_{hub} d\underline{F}^e \triangleq P_H$$

For coordinates a_1 and a_2 the associated derivative of $\underline{R}_{OV}$ is zero, and for θ the associated derivative gives a vector perpendicular to the $d\underline{F}^e$ so that the total contribution of the integrals over the hub mass is to introduce a P_H driving term to the $q_2 = X_2$ equation from (2).

Consider differential element dq of boom 1. Its inertial position vector is

$$\underline{R}_{OV} = \underline{R}_{OH} + \underline{R}_{HB} + \underline{R}_{BV} = X_1\hat{i}_1 + X_2\hat{i}_2 + r\hat{h}_1 + q\hat{b}_1^1$$

and therefore

$$\frac{\partial\underline{R}_{OV}}{\partial X_1} = \hat{i}_1\,; \quad \frac{\partial\underline{R}_{OV}}{\partial X_2} = \hat{i}_2\,; \quad \frac{\partial\underline{R}_{OV}}{\partial a_1} = q\frac{\partial\hat{b}_1^1}{\partial a_1} = q\hat{b}_2'$$

$$\frac{\partial\underline{R}_{OV}}{\partial a_2} = 0\,; \quad \frac{\partial\underline{R}_{OV}}{\partial\theta} = r\frac{\partial\hat{h}_1}{\partial\theta} + q\frac{\partial\hat{b}_1^1}{\partial\theta} = r\hat{h}_2 + q\hat{b}_2'$$

For boom 2 the analogous results are $\hat{i}_1, \hat{i}_2, 0$, $q\hat{b}_2^2$ and $-r\hat{h}_2 + q\hat{b}_2^2$. Performing the dot product of these quantities with the $d\underline{F}^e$ of (4) and integrating from ℓ_i^* to ℓ, and then adding the results for each boom together

gives the generalized forces of equation (1) as

$$
\begin{aligned}
Q_1 &= -Pl\left[\sigma_{11}\cos^2(\theta+a_1)\sin(\theta+a_1)+\sigma_{21}\cos^2(\theta+a_2)\sin(\theta+a_2)\right]\\
Q_2 &= Pl\left[\sigma_{11}\cos^3(\theta+a_1)+\sigma_{21}\cos^2(\theta+a_2)\right]+P_H\\
Q_3 &= Pl\Big\{\cos^2(\theta+a_1)\left(\sigma_{11}r\cos a_1+\tfrac{1}{2}l\sigma_{12}\right)\\
&\qquad -\cos^2(\theta+a_2)\left(\sigma_{21}r\cos a_2+\tfrac{1}{2}l\sigma_{22}\right)\Big\}\\
Q_4 &= \tfrac{1}{2}Pl^2\sigma_{12}\cos^2(\theta+a_1)\\
Q_5 &= -\tfrac{1}{2}Pl^2\sigma_{22}\cos^2(\theta+a_2)
\end{aligned}
\tag{6}
$$

where the σ_{ij} are shadow functions given by

$$
\begin{aligned}
\sigma_{11}(\theta,a_1) &= \operatorname{sgn}\left[\cos(\theta+a_1)\right]\left(1-l_1^{*}/l\right)\\
\sigma_{12}(\theta,a_1) &= \operatorname{sgn}\left[\cos(\theta+a_1)\right]\left(1-l_1^{*2}/l^2\right)\\
\sigma_{21}(\theta,a_2) &= \operatorname{sgn}\left[\cos(\theta+a_2)\right]\left(1-l_2^{*}/l\right)\\
\sigma_{22}(\theta,a_2) &= \operatorname{sgn}\left[\cos(\theta+a_2)\right]\left(1-l_2^{*2}/l^2\right)
\end{aligned}
\tag{7}
$$

5.6 The Equations of Motion

One obtains five second order differential equations for q_{i1} through q_{i5} by substituting equations (3) and (6) into (2). These equations are then linearized about a nominal spin rate ω

$$\theta = \omega t + \delta\theta$$

where a_1, a_2, $\delta\theta$, $\dot{x}_1$, $\dot{x}_2$ are assumed small quantities. Since the equations do not depend on x_1 and x_2, one need not assume that these undifferentiated variables are small. Furthermore, the linearization is done in the sense that the essential nonlinear nature of the switching times introduced by (7) in (6) is maintained, so that the equations are piecewise linear, except for the l_i^{*} dependence, between switching points in (7).

The modal variables

$$\alpha_1 = a_1 + a_2 \qquad ; \qquad \alpha_2 = a_1 - a_2$$

are introduced and the equations manipulated to eliminate the coupling with x_1, x_2 and $\delta\theta$ which is not through the Q_j. The equations are then converted to scaled time $\tau=\omega t$, and a prime used to indicate differentiation with respect to τ. The resulting equations are

$$
\begin{aligned}
\alpha_1'' + 2c_1\alpha_1' + \omega_1^2\alpha_1 &= \left[\Gamma_1(\sigma_{12}-\sigma_{22})-\Gamma_2(\sigma_{11}-\sigma_{21})\right]\left[\cos^2\tau-\delta\theta\sin 2\tau\right]\\
&\quad -\left[\Gamma_1(a_1\sigma_{12}-a_2\sigma_{22})-\Gamma_2(a_1\sigma_{11}-a_2\sigma_{21})\right]\sin 2\tau\\
\alpha_2'' + 2c_2\alpha_2' + \omega_2^2\alpha_2 &= \left[\Gamma_3(\sigma_{12}+\sigma_{22})-\Gamma_4(\sigma_{11}+\sigma_{21})\right]\left[\cos^2\tau-\delta\theta\sin 2\tau\right]\\
&\quad -\left[\Gamma_3(a_1\sigma_{12}+a_2\sigma_{22})-\Gamma_4(a_1\sigma_{11}+a_2\sigma_{21})\right]\sin 2\tau\\
&\quad -P'\cos\tau\\
\delta\theta'' + \frac{M_1}{I}\alpha_1'' &= \left[\Gamma_5(\sigma_{12}-\sigma_{22})+\Gamma_6(\sigma_{11}-\sigma_{21})\right]\left[\cos^2\tau-\delta\theta\sin 2\tau\right]\\
&\quad -\left[\Gamma_5(a_1\sigma_{12}-a_2\sigma_{22})+\Gamma_6(a_1\sigma_{11}-a_2\sigma_{21})\right]\sin 2\tau
\end{aligned}
\tag{8}
$$

where the $\sigma_{ij}(\theta,a_i)=\sigma_{ij}(\tau+\delta\theta,a_i)$ are given by (7) in which the $l_i^{*}(\theta,a_i)=l_i^{*}(\tau+\delta\theta,a_i)$ are given in (5), and the a_i are given in terms of the modal variables as

$$a_1 = \tfrac{1}{2}(\alpha_1+\alpha_2) \qquad ; \qquad a_2 = \tfrac{1}{2}(\alpha_1-\alpha_2)$$

The coefficients in these equations are

$$
\begin{aligned}
2c_1 &= c/\left[(M_3-2M_1^2/I)\,\omega\right]\\
c_2 &= \left[(M_3-2M_2^2/M)/(M_3-2M_1^2/I)\right]c_1\\
\Gamma_1 &= \tfrac{1}{2}l^2P(1-2M_1/I)/\left[(M_3-2M_1^2/I)\omega^2\right]\\
\Gamma_2 &= 2M_1rlP/\left[(M_3-2M_1^2/I)I\omega^2\right]\\
\Gamma_3 &= \tfrac{1}{2}l^2P/\left[(M_3-2M_2^2/M)\omega^2\right]\\
\Gamma_4 &= 2M_2lP/\left[(M_3-2M_2^2/M)M\omega^2\right]
\end{aligned}
\tag{9}
$$

$$
\begin{aligned}
\Gamma_5 &= \tfrac{1}{2}l^2P/(I\omega^2)\\
\Gamma_6 &= rlP/(I\omega^2)\\
P' &= 2M_2P_H/\left[(M_3-2M_2^2/M)M\omega^2\right]
\end{aligned}
$$

6. SPECIAL CASE OF NO SHADOWING AND INTERPRETATION OF EQUATIONS

If one assume that there is no shadowing the equations simplify considerably and these simplified equations will be considered here purely to gain a better understanding of the various terms. During certain short periods the sun angle on the ISEE-B spacecraft was such that there was relatively little shadowing and these equations would make a reasonable spacecraft model during those periods. Note that $l_1^{*}=l_2^{*}=0$ for no shadowing and $\sigma_{11}=\sigma_{12}$, $\sigma_{21}=\sigma_{22}$. Define case 1 as $(\sigma_{11},\sigma_{21})=(+1,+1)$, case 2 as $(-1,-1)$, case 3 as $(+1,-1)$, and case 4 as $(-1,+1)$. Note that case 1 applies for $\theta=\tau+\delta\theta$ in the range -90 to $+90$ (modulo 360°) except for some short interval at each end of the range, and case 3 applies in the range 90° to 270° except for a short interval at each end. These short intervals apply when $\cos(\tau+\delta\theta+a_1)$ and $\cos(\tau+\delta\theta+a_2)$ have different signs due to the difference in boom angles a_1 and a_2. For maximum boom angles around 3° these intervals could be at most around 6°. The equations reduce to

$$
\alpha_1'' + 2c_1\alpha_1' + \omega_1^2\alpha_1 = (\Gamma_1-\Gamma_2)\begin{cases} -\sigma_{11}(\sin 2\tau)\,\alpha_2 & \text{cases 1, 2}\\ 2\sigma_{11}\cos^2\tau - \sigma_{11}\sin 2\tau(2\delta\theta+\alpha_1) & \text{cases 3, 4}\end{cases}
$$

$$
\alpha_2'' + 2c_2\alpha_2' + \omega_2^2\alpha_2 = -P'\cos\tau + (\Gamma_3-\Gamma_4)\begin{cases} 2\sigma_{11}\cos^2\tau - \sigma_{11}\sin 2\tau(2\delta\theta+\alpha_1) & \text{cases 1, 2}\\ -\sigma_{11}(\sin 2\tau)\,\alpha_2 & \text{cases 3, 4}\end{cases}
$$

$$
\delta\theta'' + \frac{M_1}{I}\alpha_1'' = (\Gamma_5+\Gamma_6)\begin{cases} -\sigma_{11}(\sin 2\tau)\,\alpha_2 & \text{cases 1, 2}\\ 2\sigma_{11}\cos^2\tau - \sigma_{11}\sin 2\tau(2\delta\theta+\alpha_1) & \text{cases 3, 4}\end{cases}
$$

Consider cases 1 and 2 which apply nearly all the time. The righthand side of the α_1 equation is essentially a linear term with a periodic coefficient which could be included as part of the homogeneous equations of the system which now are coupled. The same is true of the $\delta\theta$ equation, and of two of the terms for the α_2 equation. Then, if the short intervals of around 6° are neglected, only the α_2 equation has a true forcing function. The P' term represents the excitation of the α_1 mode when the hub is accelerated due to radiation pressure, and the $2\sigma_{11}\cos^2\tau$ term can be understood by examination of Figure 7a. The radiation pressure tries to increase a_1 and decrease a_2 so that the force on α_2 is positive. If θ is rotated by 180° the roles of a_1 and a_2 reverse, σ_{11} changes sign, and the radiation pressure tries to decrease α_2 as this term predicts.

To understand the terms that drive the α_1 equation, which is the mode of interest in the spin ripple, consider Figure 7 a, and note that it corresponds to $\alpha_2 > 0$, $\sigma_{11} = +1$ and a τ corresponding to a θ in the first quadrant. The radiation pressure tries to increase a_1 and decrease a_2, but because of the positive α_2, the projected area of boom 1 is smaller than the projected area of boom 2, and hence the force trying to increase a_1 is smaller than the force trying to decrease a_2 with the net effect that $\alpha_1 = a_1 + a_2$ should see a negative force, i.e. $-\sigma_{11}(\sin 2\tau)\alpha_2$.

If α_2 is negative the effect reverses, and if τ is made negative so that Θ is between -90° and 0° the effect reverses consistent with the sign of $\sin 2\tau$, and if Θ is rotated into the third quadrant the a_1 and a_2 roles interchange and the effect reverses consistent with the sign of σ_{11}.

Cases 3 and 4 can be studied with the aid of Figures 7b and c. In b, $\tau \approx 90^\circ$, $\sigma_{11} = -1$ and the radiation force tries to decrease a_1 and a_2 giving the negative forcing term $2\sigma_{11}\cos^2\tau$. To investigate dependence on $\delta\theta$ consider part c of the figure for which τ is somewhat less than 90°. By increasing $\delta\theta$, the force on a_1 increases and on a_2 decreases but to a lesser extent, so the term $-\sigma_{11}\sin 2\tau\,(2\delta\theta)$ is positive. Similarly increasing α_1, by changing a_1 by Δa_1 and a_2 by Δa_2 as illustrated, has the same effect. If τ is above 90° the trend reverses as is consistent with the sign of $\sin 2\tau$, and if τ is increased by 180° the roles of a_1 and a_2 reverse and the σ_{11} sign changes appropriately.

7. POSSIBLE SOLUTION METHODS

Consider several approaches to the study of the oscillations predicted by equation (8). The basic difficulty is that a steady oscillation is sought, but the differential equation solution will also contain a transient part which decays with a 6 day time constant. If the damping is artificially increased to cause the solution to convergence more quickly to a steady oscillation, the oscillation itself is strongly affected and one converges to an oscillation of the wrong amplitude, or if a limit cycle is involved the desired steady oscillation may disappear.

In order to apply any analytical approaches, the equations should be simplified as much as possible. Evaluation of the coefficients in equation (8) gives

$$\Gamma_1 = 0.1888 \times 10^{-6} \qquad \Gamma_5 = 0.9282 \times 10^{-8}$$
$$\Gamma_2 = 0.1920 \times 10^{-8} \qquad \Gamma_6 = 0.8142 \times 10^{-9}$$
$$\Gamma_3 = 0.1879 \times 10^{-6} \qquad P' = 0.2108 \times 10^{-8}$$
$$\Gamma_4 = 0.1260 \times 10^{-9}$$

Since $\Gamma_2, \Gamma_4, \Gamma_5, \Gamma_6$ and P' are much smaller than Γ_1 and Γ_3 one could eliminate all but the Γ_1 and Γ_3 terms, and eliminate $\delta\theta$ by $-(M_2/I)\alpha_2$. It would be desirable to have a simpler form for the functions ℓ_1^* and ℓ_2^*. One possibility is to assume that they switch from 0 to ℓ in one step occurring at some point $\tau + \delta\theta + a\tau = \pi/2 - \epsilon$ or $3\pi/2 - \epsilon$ for some ϵ and then back to zero at $\pi/2 + \epsilon$, $\frac{3\pi}{2} + \epsilon$. With this choice

$$\alpha_1'' + 2c_1\alpha_1' + \omega_1^2\alpha_1 + 2\Gamma_1 \sin\tau\,|\cos\tau|\,\alpha_2$$
$$= \begin{cases} -\frac{1}{2}\sigma_{22}\Gamma_1\left[2\cos^2\tau - \sin 2\tau\,(\alpha_1 - \alpha_2 + 2\delta\theta)\right] \\ \quad + \sigma_3\Gamma_1(\sin 2\tau)\,\alpha_2 & \text{if } \sigma_{12} = 0 \\ +\frac{1}{2}\sigma_{12}\Gamma_1\left[2\cos^2\tau - \sin 2\tau\,(\alpha_1 + \alpha_2 + 2\delta\theta)\right] \\ \quad + \sigma_3\Gamma_1(\sin 2\tau)\,\alpha_2 & \text{if } \sigma_{22} = 0 \\ 0 & \text{otherwise} \end{cases}$$

$$\alpha_2'' + 2c_2\alpha_2' + \omega_2^2\alpha_2 + 2\Gamma_3\,|\cos\tau|\,\sin\tau\,(\alpha_1 + 2\delta\theta)$$
$$= 2\Gamma_3|\cos\tau|\cos\tau + \begin{cases} \frac{1}{2}\sigma_{22}\Gamma_3\left[2\cos^2\tau - \sin 2\tau\,(\alpha_1 - \alpha_2 + 2\delta\theta)\right] \\ \quad + \sigma_3\Gamma_3\left[2\cos^2\tau - \sin 2\tau\,(\alpha_1 + 2\delta\theta)\right] & \text{if } \sigma_{12} = 0 \\ \frac{1}{2}\sigma_{12}\Gamma_3\left[2\cos^2\tau - \sin 2\tau\,(\alpha_1 + \alpha_2 + 2\delta\theta)\right] \\ \quad + \sigma_3\Gamma_3\left[2\cos^2\tau - \sin 2\tau\,(\alpha_1 + 2\delta\theta)\right] & \text{if } \sigma_{22} = 0 \\ 0 & \text{otherwise.} \end{cases}$$

where $\sigma_3 = \text{sgn}[\cos(\tau)]$ and where it is assumed that ϵ is wide enough that $\sigma_{12}\sigma_{22}$ is never negative. Note that periodic coefficient terms have been added to both sides of the equations in order to make the bracketed "forcing function" on the right hand side zero unless one of the booms is in the ϵ shadow region. One expects that the small periodic coefficient terms will have only a very small effect on the solution to the "homogeneous" equations (i.e. with the right hand sides set to zero), so that these terms could be dropped and concentration placed on the small kicks given to each equation when σ_{12} or σ_{22} is zero.

The small intervals for which $\sigma_{12} = 0$ or $\sigma_{22} = 0$ suggest approximating the bracketed terms by impulses. This could be done by evaluating the solution of the equations at $(2n-1)\pi/2$ without these terms, using a Taylor series expansion of the solution to determine the interval for which σ_{12} or σ_{22} is zero, and then integrating the term over this interval to generate the area to use under the impulse which would be applied at $(2n-1)\pi/2$ or more accurately at the midpoint of the $\sigma_{12} = 0$ or $\sigma_{22} = 0$ time interval (or more accurately still, a set of impulses can be made for the periods when σ_{12} and σ_3, or σ_{22} and σ_3 do not change sign). The number of terms involved in this approach becomes large.

It is also natural in problems of this nature to consider averaging methods. If one assumes that the period of the oscillations of interest are long compared to the spin period, which is somewhat questionable in this problem where the ratio is 4.37, then one might assume that α_1 and α_2 are constant over each spin period for the nonlinear terms. This approach might be more natural in the original equations (8). When applied to the simplified equations, the approach results in essentially the impulse approach discussed above.

The contribution of each impulse could be distributed over the half rotation between each impulse. If this is done a large number of terms are generated, including terms like

$$\alpha_1'' + 2c_1\alpha_1' + \omega_1^2\alpha_1 = -\Gamma\epsilon^2\alpha_1\alpha_1'$$

Consider the possibility of a limit cycle in such an equation. If $\alpha_1 = A\cos\bar{\omega}\tau$ is the fundamental

frequency in the limit cycle, then the product $\alpha_1\alpha_1'$ will generate a contribution to α_1, at frequency $2\bar{\omega}$. Letting $\alpha_1 = A\cos\bar{\omega}\tau + B\cos(2\bar{\omega}\tau+\phi)$ one can substitute into the equation to find an A,B, $\bar{\omega}$ and $\emptyset$ for which the equation is satisfied for these two frequencies. Note that is c_1 is very small the limit cycle frequency $\bar{\omega}$ should be near but not equal to the resonant frequency ω_1. One expects the limit cycle to be unstable since too small an amplitude in α_1, precludes the nonlinear term, with $(\Gamma\epsilon^3\alpha_1)$ considered as a coefficient, from dominating the damping term with 2c as coefficient. Including other nonlinear terms on the right hand side, for example there will be cubic and fourth order terms in α_1 and α_1' which might produce an additional stable limit cycle at a larger amplitude. Such a result would be consistent with the observed behaviour of the satellite, which failed to exhibit the spin ripple until the first spin rate manoeuvre in deployed configuration was performed, and has exhibited the spin ripple ever since. This behaviour would correspond to initial conditions within the stable limit cycle originally so that α_1 converged to zero, and outside this limit cycle after the manoeuvre so that the oscillations grew to the stable limit cycle. Unfortunately, the great plethora of nonlinear terms obtained by this approach precludes following the approach to a conclusion.

A final possible analytical approach is to use the correct ℓ_i^* in equations (8) but employ the remaining simplifications. Then search for a limit cycle $\alpha_1 = A_1\cos\bar{\omega}t$, $\alpha_2 = A_2\cos(\bar{\omega}t+\phi_2)$, plus other frequency terms as needed, determine the appropriate frequency components for each term of the equation with these solutions substituted, and then solve for the amplitudes, phase angles, and the fundamental frequency itself. This direct approach to search for a limit cycle is again intractable analytically.

8. NUMERICAL RESULTS

In the absence of an effective analytical approach, a computer simulation of the differential equations (8) was generated.

In order to avoid the problem of selecting the initial conditions on $\delta\theta$ for which the chosen nominal spin rate ω is the average spin rate, and in accordance with the small size of Γ_5 and Γ_6, $\delta\theta$ was set equal to $-(M_1/I)\alpha_1$ (even if the right hand side of the $\delta\theta$ equation averages to zero, $\delta\theta$ will still generally have a secular growth or decay term unless the initial conditions are chosen judiciously, and $\delta\theta$ was assumed to be small in the derivation of the equations).

The fact that the damping in the system has a 6 day time constant precludes searching for a periodic limit cycle by choosing various initial conditions and integrating until the transients have decayed to a negligible level. If the equations are thought of as linear equations with a forcing function on the right hand side in (8), then to obtain that particular solution without any transient contribution from the solution to the homogeneous equation, the initial conditions can be set to zero at some point for which the forcing functions are all zero. Hence, runs were made with the initial conditions specified as zero at $\tau = \pi/2$. The results are shown in Figures 8 and 9. The amplitude of the oscillations, given in degrees, are very small, indicating that if the spin ripple is a result of the solar radiation pressure excitation being investigated, its amplitude is not determined by the simple response of the α_1 equation driven by a forcing function containing a component at the resonant frequency. Rather, if the equations are to predict the spin ripple, they could only do so as an essentially nonlinear phenomenon, i.e. as a limit cycle.

Figures 10, 11 and 12 study the excitation of α_1 due to a sizable α_2 oscillation. The initial conditions for α_1 were set to zero, and the initial conditions on α_2 set to 7.5° with a zero derivative. The response of α_1 is still very small as shown in Figure 10. The "forcing function", i.e. the right hand side of the α_1 equation is plotted in Figure 11. Figure 12 shows the 7.5° oscillation of α_2 together with its "forcing function".

A long computer simulation was made to try to make equations (8) predict the increase in spin ripple amplitude after a spin ripple reduction manoeuvre. The initial condition on $\delta\theta$ was set to 0.1°, which corresponds to an α_1 of 2°. A step size of 20° of rotation was used except within 10° of the 90° and 270° (modulo 360°) points where a step size of 4° was used. A fourth order Runga Kutta integration routine was used, and 6000 seconds of real time simulated. The ISEE-B data over this period of time exhibited a measurable increase in the spin ripple amplitude of 1%. The initial condition α_2 was set to 3° with a zero initial derivative. Of course, there is no data to guide this choice, and in the search for a limit cycle, proper selection of initial conditions could be critical. Unfortunately, the amount of computer time needed precludes a systematic search for a limit cycle. The simulation results showed a slight decay in both α_1 and α_2, in the former case a decay of about 2%, instead of the expected spin ripple growth.

9. CONCLUSION

In summary, the numerical computation of the solar radiation pressure excitation have failed to predict the observed spin ripple behaviour. The results are inconclusive in two senses. First, a limit cycle can depend critically on size and phasing of the initial conditions and only one set of initial conditions was investigated, and secondly, if the exact points at which the signum functions σ_{ij} switch values are important, the relatively coarse integration step size could have failed to see this contribution. With this priviso the results appear to indicate that the solar radiation pressure alone is insufficient to predict the observed behaviour, and other possible mechanisms should be sought.

After this work was completed, additional data indicated that although no striking change in spin ripple amplitude appeared near perigee, the spin rate istself is affected. Implications of these data are being investigated.

ACKNOWLEDGEMENTS

The Authors would like to acknowledge A. Schütz for his contributions in generating numerical results.

9. REFERENCES

1. Fedor, J.V., The Effect of Solar Radiation Pressure on the Spin of Explorer XII, NASA TN D-1855, August 1963.

2. Etkin, B. and P.C. Hughes, "Explanation of the Anomalous Spin Behaviour of Satellites with Long, Flexible Antennae", Journal of Spacecraft and Rockets, Vol. 4 No. 9, September 1967, pp. 1139-1145.

3. Vigneron, F.R., "Dynamics of Alouette ISIS Satellites", Astronautica Acta, Vol. 18, No. 3, 1973, pp. 201-213.

4. Vigneron, F.R., D. Harrison, and G. Bower, "Spin Rate Behaviour of ISIS-I," Journal of Spacecraft and Rockets, Vol.8, No. 10, October 1971, pp. 1099-1101.

5. Chambaz, B., L. Fraiture, and N. Wiengarn, "Irregularities in the Motion of Spin Stabilized Earth Satellites", Proceedings of the Symposium on Spacecraft Flight Dynamics, Darmstadt, May 1981.

6. Proceedings of the Symposium on Gravity-Gradient Attitude Stabilization, Aerospace Corporation, El Segundo, California, U.S. Air Force SAMSO-TR-69-307, September 1969.

7. Tsuchiya, K., "Attitude Behaviour of a Dual Spin Spacecraft Composed of Asymmetric Bodies," Journal of Guidance and Control, Vol. 2, No. 4, 1979, pp. 328-333.

8. Likins, P.W. and H.K. Bouvier, "Attitude Control of Nonrigid Spacecraft", Astronautics and Aeronautics, Vol. 9, 1971, pp. 64-71.

9. Frank, W., A. Hawkyard, and D. Eaton, ISEE-B System Data Summary for Operations, ESTEC Document, ISEE-MB-3438, 1977.

10. Massart, J.A., A. Schutz and A. Thiery, "ISEE-B Spin Ripple Damping", ESOC ISEE-B Flight Dynamics Report III, Part A, 1979.

11. Thiery, A., "Implementation of Spin Ripple Damping Software at GSFC", ESOC ISEE-B Flight Dynamics Report, 1980.

12. Crellin, E.B., and R.H. Dennett, ISEE-B Spacecraft Dynamic Analysis, British Aircraft Corporation BAC/TN73611/14263, 1975.

13. Massart, J.A., Theoretical and Practical Considerations on the Damping of ISEE-B Spin Ripple, European Space Operations Center, ESOC-OAD-WP-156, 1979.

14. Tsuchiya, K., "Thermally Induced Nutational Body Motion of a Spinning Spacecraft with Flexible Appendages", AIAA Journal, Vol. 13, No. 4, April 1975, pp. 448-453.

15. Vigneron, F.R., and A.P. Boresi, "Effect of the Earth's Gravitational Force on the Flexible Crossed-Dipole Satellite: Part I - Configuration Stability and Despin", Canadian Aeronautics and Space Institute Transactions, Vol. 3, No. 2, September 1970, pp. 115-126.

16. Vigneron, F.R., and T.W. Garrett, "Solar Induced Distortion - Atmospheric Drag Coupling in Alouette Satellites", Defense Research Board, DRTE Report No. 1171, Ottawa, Canada, 1967.

17. Vigneron, F., "Thin-Walled Beam Theory Generalized to Include Thermal Effects and Arbitrary Twist Angle", Department of Communications, Ottawa, Canada, CRC Report No. 1253, October 1974.

Table 1. Nominal Orbit and Attitude Parameters

Orbital Parameters

epoch	30 April 1981 at 12h 38 min 03 sec
semi-major axis	75602.68 km
eccentricity	.890851
inclination	48.543°
mean anomaly	0.623°
argument of perigee	15.601°
motion	+ 0.0243°/day
R.A. of ascending mode	358.770°
motion	- 0.0270°/day
anomalistic period	2.3944344 days
height of perigee	1873.85 km
height of apogee	136575.24 km

Attitude Parameters (the spin axis is kept aligned with the north perpendicular to the ecliptic plane within a 3 deg. cone).

spin axis right ascension	270.0°
spin axis declination	66.3°
angle spin axis - sun direction	90.0°
control tolerance	(- 1.0°,+3.0°)
spin period	3.03 sec
control tolerance	(- 0.0154 sec, + 0.0154 sec)

Table 2. Geometric - Thermal - Mass Properties (Ref. 9)

1. Cylindrical Hub radius 0.635 m
   height 1.14 m

	solar cells	skirt
reflectivity coefficient	0.19	0.04
height	0.85 m	0.29 m

2. Hinge Booms

radius	~ 0.03 m		
length	2.27 m	2.29 m	2.15 m
reflectivity coefficient	0.89		

3. Wire Booms

length	~ 14.477 (±0.02) m
width	0.005 m
thickness	0.0004 m
linear density	0.00134 kg/m
attachment point radius taken as	0.635 m
distance hub center to spool center	0.590 m
reflectivity coefficient	0.55

4. Masses (midlife value)

total	152.4 kg
tip masses	0.01594 kg(along- X axis)
	0.01575 kg(along+ X axis)

5. Position of Center of Mass

Stowed Wires	Fully Depolyed
X = 0.009 m	X = 0.01 m
Y = 0.008 m	Y = 0.01 m
Z = 0.336 m	Z = 0.33 m

6. Principal of Inertia

Stowed Wires	Deployed Wires
I_{zz} 83.1 kgm^2	94.7 kgm^2
I_{yy} 52.9 kgm^2	63.3 kgm^2
I_{xx} 49.9 kgm^2	51.0 kgm^2

7. Principal Axes Direction

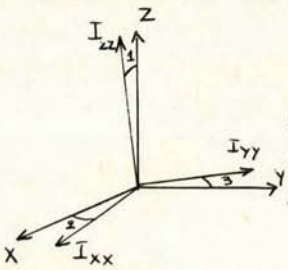

Stowed Wires	Deployed Wires
∠1 0.00°	∠1 0.01°
∠2 42.56°	∠2 7.13°
∠3 42.	∠3 7.13°

8. Magnetic Moment

0.037 Am^2

Table 3. Satellite Data

Raw Satellite Data Sun Transit Times (Clock Counts)		Spin Period (Counts)		Sun Elevation Information (Counts)
Meridian	Oblique	Meridian	Oblique	
t_i^m	t_i^o	$t_{i+1}^m - t_i^m$	$t_{i+1}^o - t_i^o$	$t_i^o - t_i^m$
35893	35840	12415	12415	- 53
48321	48268	12428	12428	- 53
60754	60701	12433	12433	- 53
7640	7587	12422	12422	- 53
20054	20001	12414	12414	- 53
32477	32424	12423	12423	- 53
44910	44857	12433	12433	- 53
57337	57284	12427	12427	- 53
4217	4164	12416	12416	- 53
16634	16581	12417	12417	- 53
29065	29012	12431	12431	- 53
41497	41444	12432	12432	- 53
53915	53862	12418	12418	- 53
794	741	12415	12415	- 53
13220	13167	12426	12426	- 53
25654	25601	12434	12434	- 53
38077	38024	12423	12423	- 53
50491	50438	12414	12414	- 53
62912	62859	12421	12421	- 53
9809	9756	12433	12433	- 53
22238	22185	12429	12429	- 53
34654	34601	12416	12416	- 53
47070	47018	12416	12417	- 52
59500	59447	12430	12429	- 53
6396	6343	12432	12432	- 53
18817	18764	12421	12421	- 53
31231	31178	12414	12414	- 53
43655	43602	12424	12424	- 53
56089	56036	12434	12434	- 53
2978	2925	12425	12425	- 53
15393	15340	12415	12415	- 53
27812	27759	12419	12419	- 53
40244	40191	12432	12432	- 53
52674	52621	12430	12430	- 53
65091	65038	12417	12417	- 53

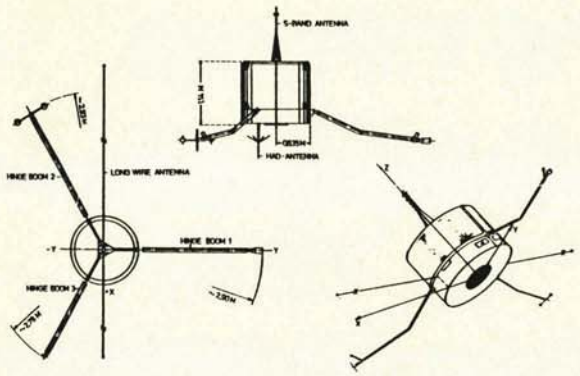

Figure 1. ISEE-B Spacecraft Configuration

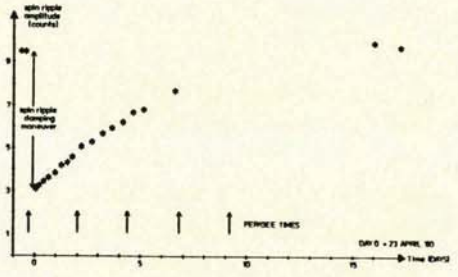

Figure 4. Evolution of Spin Ripple Amplitude following the second spin ripple reduction maneuver

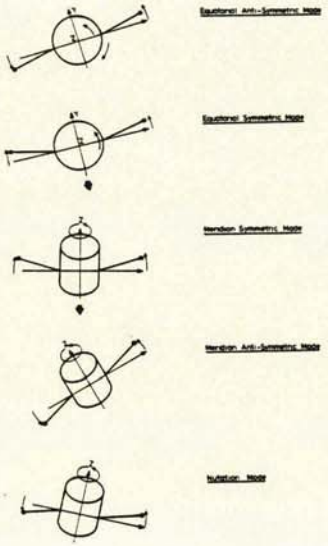

Figure 2. The Normal Modes of Vibration

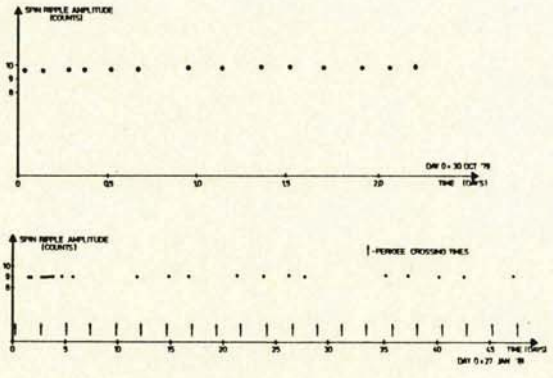

Figure 5. Evolution of Spin Ripple Amplitude

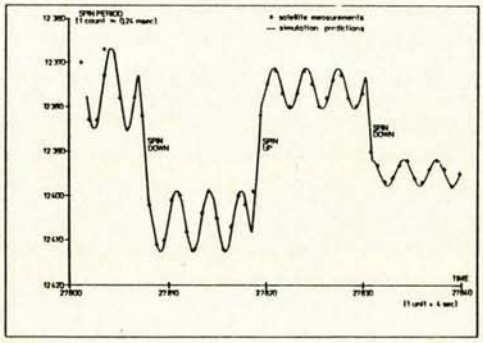

Figure 3. Spin Ripple Damping Maneuver

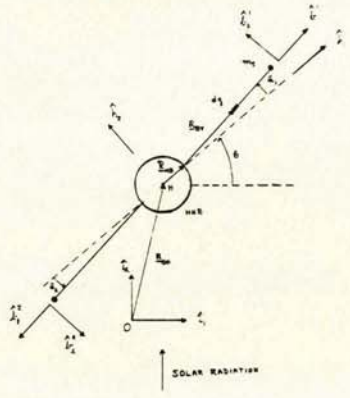

Figure 6. Reference Frames and Position Vectors

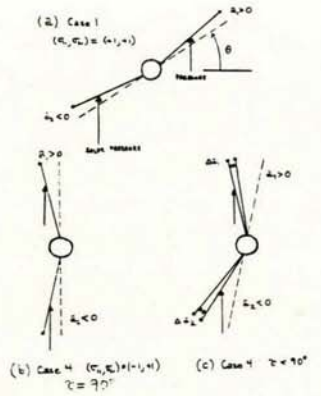

Figure 7. Interpretation of the Forcing Function

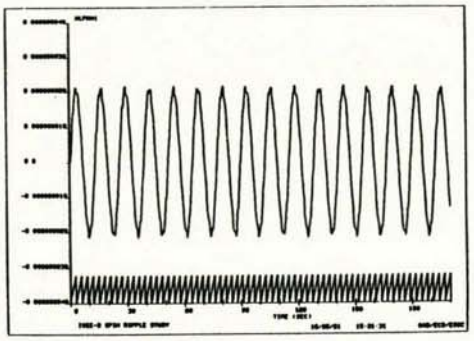

Figure 8. Solution for α_1, with Zero Initial Conditions at $\pi/2$

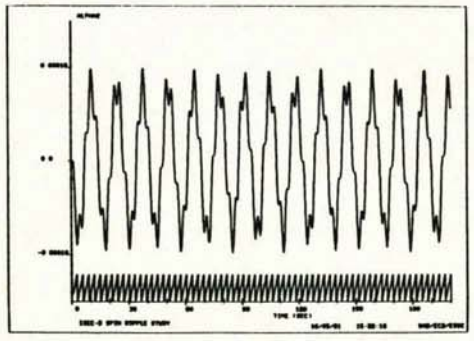

Figure 9. Solution for α_2 with Zero Initial Conditions at $\pi/2$

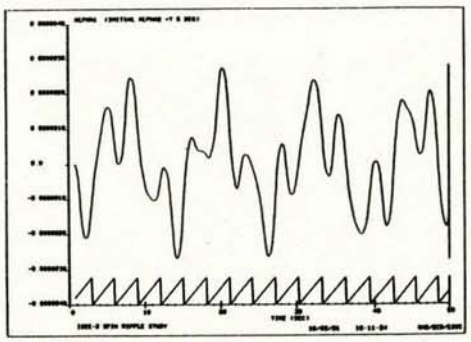

Figure 10. Response of α_1, to a 7.5° Initial Value of α_2

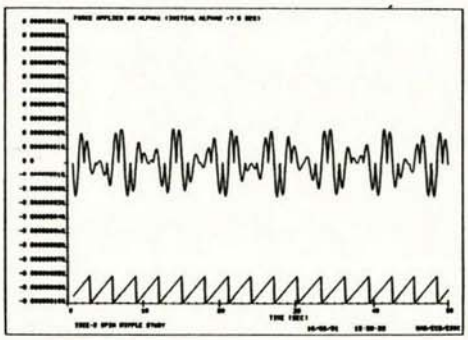

Figure 11. The Driving Terms to the α_1 Harmonic Oscillator Equation

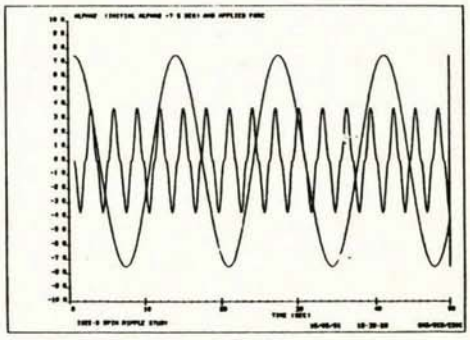

Figure 12. The Solution for α_2 with a 7.5° Initial Value, and the associated α_2 driving term